Doppler Spread Analysis of Human Motions for Body Area Network Applications

Ruijun Fu, Yunxing Ye, Ning Yang, Kaveh Pahlavan
Center for Wireless Information Network Studies
Department of ECE, Worcester Polytechnic Institute, Email: {rjfu,yunxingye,nyang,kaveh}@wpi.edu

***Abstract*—Many current and future medical devices are wearable and the human body is used as a carrier for wireless communication, which implies that the human body is a crucial part of the transmission medium in Body Area Networks (BANs). In order to understand the propagation characteristics of the human body, it is imperative to analyze the Doppler spread spectrum, which is caused by human body motions. Using a network analyzer, Doppler spreads and coherence time of temporal variations caused by human body motions can be measured and analyzed using a single tone waveform for different scenarios in a shielded room. From the narrowband measurement results, the Doppler spread varies approximately from $0.6Hz$ to $12Hz$ for different scenarios, the RMS Doppler bandwidth is in the range from $0.6Hz$ to $4Hz$, and the coherence time differs from $20ms$ to $1s$, all of which are measured at the Medical Implant Communication Service (MICS) band, the Industrial Scientific Medical (ISM) band and the Ultra-Wideband (UWB) band. Root mean square fittings of three different functions to received signal strength measurements were performed for different scenarios. Results show that the Gaussian function generally provides a good fitting model, which is independent of center frequencies.**

I. Introduction

Rapid growth in low power integrated circuits and wireless communication has made medical detections with miniaturized sensors come true. These wearable and swallowable medical sensors have earned an increasing market in recent years, where real time health monitor systems attract a lot of attention. IEEE 802.16.5 Task Group 6 is officially working on the standardization for wireless Body Area Networks and focusing on multiple issues including propagation characteristics, power consumption and security. But there are still many challenges in Body Area Networks, which call for the increased mobility, the higher capacity and the lower power consumption. In order to design better receivers for medical applications, it is significant to understand the propagation characteristics in, on and around the human body.

The propagation characteristics of dynamic channels caused by human body motions have been researched in recent studies[2−8]. The considered frequency bands include the MISC band, the ISM band, the WMTS (Wireless Medical Telemetry) band and the UWB band. Measurements related to dynamic channels were conducted in an anechoic chamber room, an office room and a hospital room by either a channel sounder using wideband measurements or a Vector Network Analyzer (VNA) using narrowband measurements. Some of the past researches are the analysis of on-body propagation effects, including the path loss (PL) models[16,21] for a variety of scenarios CM1∼CM4[20] around $400MHz$, $600MHz$, $900MHz$, $2.4GHz$, and $5.0GHz$. Other previous papers are concentrated on the statistical characterization of channels for a given scenario by attaching a probability density function (pdf)[5] or second-order statistics[7] including the level crossing rate and the fade duration. Additionally, discussion about the channel temporal stability is readily given in [14-15]. But none of these papers above have discussed the temporal variations of the on-body channel derived from the Doppler spread spectrum aspect. Furthermore, the existing body posture detection is either based on the videos or images taken by a camera[21] or wearable sensors using accelerometry[22]. Based on the statistical characterization, we could also use the Doppler spread to detect different human body motions.

In this paper, we focused on the propagation characteristics of the dynamic on-body channels induced by three continuous human body motions. The Doppler spread spectrum, the RMS Doppler bandwidth and the shape of Doppler spread spectrum are analyzed based on the narrowband measurements with a Vector Network Analyzer. The Doppler spread is defined as the width of received spectrum when a single tone waveform has been transmitted, which could provide information about the fading rate of the channel. The RMS Doppler bandwidth is used to describe the distribution of power compared with Doppler spread. Both the Doppler spread and the RMS Doppler bandwidth are of great importance to determine the maximum signalling rate allowable for coherence demodulation, to improve detection and to optimize transmission at the physical layer. And Coherence time, which is one of crucial parameters for evaluation and implementation of potential wireless systems is also required to be analyzed and discussed thoroughly. In this study, we did a comprehensive discussion about the Doppler spread effects caused by standing, walking and jogging motions at the MICS, ISM and UWB bands in Body Area Networks.

The remainder of this paper is organized as follows. Measurement environment, measurement equipment and on-body measurement scenarios are described in section II. Section III presents the analysis of the Doppler effects for different scenarios mentioned in section II. A set of time domain waveform and the frequency spectrum are also given visually to compare the Doppler spread for different human body motions. In section IV, the RMS Doppler bandwidth is described to further discuss the distribution of received power. Section V shows

978-1-4577-1348-4/11/$26.00 ©2011 IEEE

the shape fittings of the Doppler spread spectrum. Finally, coherence time, which is the time domain dual of the Doppler spread is used to characterize the time domain varying nature of the on-body channels.

II. Measurement Setup

The on-body to on-body channel measurements were performed by using two antennas placed on a test subject in a shielded room with a size of $2.32m \times 2.41m \times 2.29m$, which could prevent the entry of outside signals or the escape of reflected signals inside. Three sets of wearable antennas are used during the measurements, all of which are omnidirectional, working at around $400MHz$, $2.25GHz$ and $4.5GHz$ separately within MICS, ISM and UWB bands. Antennas used for $400MHz$ narrowband measurements are a loop antenna at the receiver and a helical antenna at the transmitter; monopole antennas, working in a frequency band from $2.1GHz$ to $2.4GHz$, are designated to send $2.25GHz$ single tone waveform from the transmitter to the receiver; and patch antennas (SkyCross^{TM} SMT-3TO10M-A) are used to send and to receive a $4.5GHz$ single tone waveform.

Short time variations of the radio channel are measured by an Agilent E8363B Vector Network Analyzer (VNA). A continuous single tone waveform at $400MHz$, $2.25GHz$, and $4.5GHz$ with a transmission power of $0dBm$ is generated separately from the TX port of the VNA and received at the RX port in time domain. The IF bandwidth is configured to be $3kHz$. The forward transmission coefficient ($S21$), measured and stored in PC real time, is analyzed and evaluated off-line. In the 20 sec interval, the network analyzer took samples of received signal strength at a rate of 80 samples/sec. Therefore the maximum Doppler shift measurable is $40Hz$, and the resolution is $0.012Hz$.

All measurements were based on different human body motions, where transmitting and receiving antennas were attached to different positions of the human body. By using a scenario-based approach[19], a scenario set, denoted by $S = \{Freq, Motion, TX, RX\}$, is composed of a frequency set $Freq$, a motion set $Motion$, two antenna position sets TX and RX. In the motion set, three kinds of human postures were considered: standing still, walking and jogging on a spot, denoted by $Motion = \{Stand, Walk, Jog\}$. Only respiration and palpitation occur when the human body is standing still. In the walking scenario, the human body is expected to walk with arms and feet moving periodically and slowly in a small range. When the human body is jogging, both arms and feet move very quickly, which would cause a greater channel variation. The frequency set $Freq$ is composed of $Freq = \{400MHz, 2.25GHz, 4.5GHz\}$, where the increasing center frequency of transmitters would also impact the small scale fading characteristics of Body Area Network channels.

The transmitting and receiving antennas are placed on different positions on the test subject's body. The receiver is attached to the right hip of test subject which is denoted by $RX = \{RightHip\}$, since the receiving sensor is often considered to be placed on the belt for either in-body or on-body transmitter in current medical applications. And the position of transmitter is denoted as $TX = \{\text{Back}, \text{Chest}, \text{LeftWrist}, \text{LeftAnkel}, \text{RightAnkle}\}$. Fig.1(a) illustrates the lay-out of shielded room and fig.1(b) shows antenna positions on the tested subject.

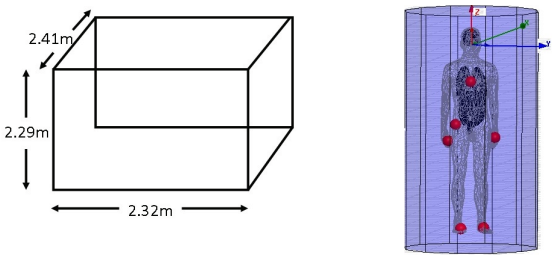

(a) (b)

Fig. 1: Measurement Environment (a) The Shielded Room (b) Antenna Positions.

III. Doppler Spreads

It is well known that an apparent change of frequency will occur in radar systems if there is a relative motion between the transmitter and the receiver. On one hand, whenever the source waves move towards the receiver, the receiver will detect a higher frequency sound, which is an upward shift in frequency. The reason is that the receiver receives more waveforms per second and considered this observation as a higher frequency. On the other hand, the receiver will perceive a lower frequency sound when either the transmitter or receiver moves away from each other, since the receiver will detect a less number of waveforms, which will result in a downward shift in frequency. The maximum Doppler frequency shift f_m is determined by the velocity of the movement v_c and the length of propagation wave $\lambda = \frac{c}{f_c}$ as

$$f_m = \pm \frac{v_c}{\lambda}, \tag{1}$$

where $c \approx 3 \times 10^8 m/s$ is the velocity of light and f_c is the transmission center frequency. When either the transmitter or the receiver both moves toward each other, the Doppler frequency shift f_m would be positive. Conversely, f_m would be negative if transmitter moves away from the receiver. Hence, the maximum value of f_m could be approximated from the Doppler spread B_D of the on-body to on-body communication.

From the narrowband measurement results, we have the time domain response $H(f_c; t)$ received from an unmodulated sine wave transmitted at $400MHz$, $2.25GHz$ and $4.5GHz$ respectively. By design, each measurement is a sample of an ergodic process and stationary for a certain period. All the following analysis below assumes that the channel is wide-sense stationary (WSS) at a minimum[2].

After the Fourier transform of the time domain data $H(f_c; t)$, the Doppler spread $D(\lambda)$ could be calculated by applying a threshold of $-10dBm$ in the frequency domain, where $D(\lambda) = \int_{-\infty}^{\infty} H(f_c; t) e^{-j2\pi\lambda t} dt$.

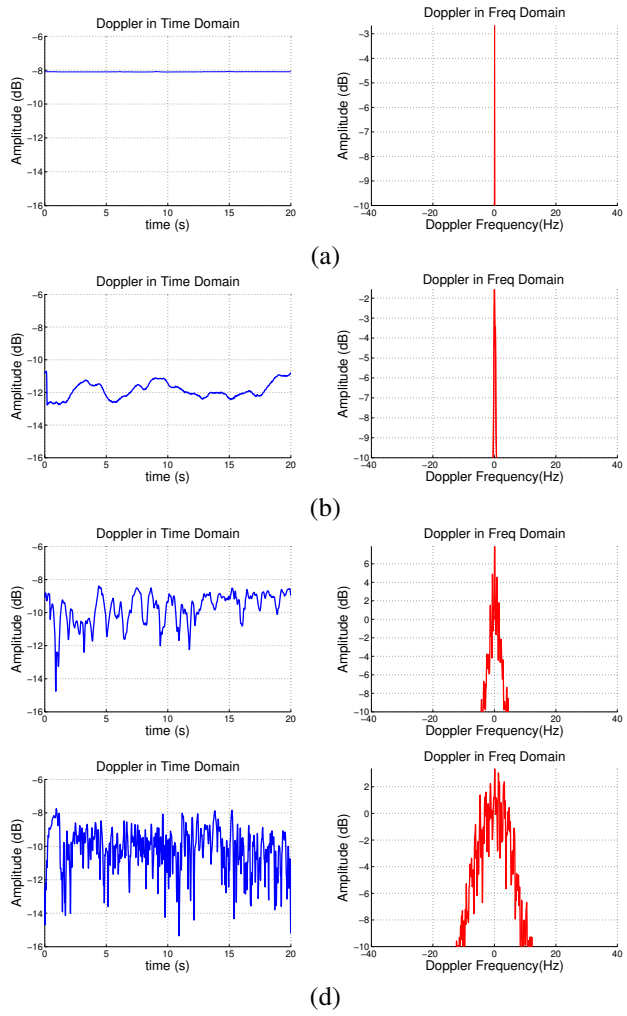

Fig. 2: Doppler Spread in Time Domain and Frequency Domain for Different Human Body Motions (a) Freespace (b) Stand Still (c) Walk On a Spot (d) Run On a Spot

A set of Doppler spreads for a specific scenario $S1 = \{Freq1, Motion1, TX1, RX1\}$ is shown in Fig.2, including both time domain response $H(f_c;t)$ and corresponding response $D(\lambda)$ in frequency domain. In this specific case, we have $Motion1 = \{Stand, Walk, Jog\}$, $Freq1 = \{2.25GHz\}$, $TX1 = \{LeftAnkle\}$ and $RX1 = \{RightHip\}$. The Doppler spreads for standing, walking and jogging motions are approximately $0.6758Hz$, $2.929Hz$ and $11.19Hz$ for the communication link between left ankle and right hip.

For the on-body to on-body measurements, the Doppler spread varies approximately from $0.6Hz$ to $12Hz$ for scenario set $S = \{Freq, Motion, TX, RX\}$, which is caused by a frequency set $Freq$, a motions set $Motion$ and antenna position sets TX and RX. Table I lists a summary of Doppler spreads for a specific scenario set $S2 = \{Freq2, Motion2, TX2, RX2\}$, where $Freq2 = \{2.25GHz\}$, $Motion2 = \{Stand, Walk, Jog\}$, $TX2 = \{Back, Chest, LeftWrist, LeftAnkle, RightAnkle\}$ and $RX2 = \{RightHip\}$. From table I we can conclude that the Doppler spread increases from $0.676Hz$ to $11.190Hz$ as the body posture changes and the position of TX antenna changes. For the standing motion, the Doppler spread is always below $1Hz$ since the channel fading is caused by small body movements. And the channel remains to be constant for a longer period. In the walking and jogging scenarios, the Doppler spread varies around $4Hz$ and $9Hz$ separately. The variation of Doppler spread is also affected by the speed of walking or jogging. As the transmission antenna moves far away from the receiver attached to the right hip, the Doppler spread rises in a small range.

TABLE I: Doppler Spreads and RMS Doppler Bandwidth for Human Body Motions at Different Transmission Range

Motion	TX	Doppler Spread	RMS Bandwidth
Stand	Chest	0.826 Hz	0.8673 Hz
Stand	Back	0.876 Hz	0.776 Hz
Stand	Left Wrist	0.826 Hz	0.698 Hz
Stand	Left Ankle	0.676 Hz	0.7696 Hz
Stand	Right Ankle	0.727 Hz	0.983 Hz
Walk	Chest	4.781 Hz	1.899 Hz
Walk	Back	4.981 Hz	2.209 Hz
Walk	Left Wrist	4.481 Hz	2.061 Hz
Walk	Left Ankle	4.631 Hz	2.2471 Hz
Walk	Right Ankle	4.281 Hz	2.006 Hz
Jog	Chest	9.937 Hz	2.898 Hz
Jog	Back	9.287 Hz	2.728 Hz
Jog	Left Wrist	9.587 Hz	3.115 Hz
Jog	Left Ankle	11.190 Hz	3.008 Hz
Jog	Right Ankle	10.690 Hz	3.184 Hz

TABLE II: Doppler Spreads and RMS Doppler Bandwidth for Human Body Motions at Different Transmission Frequency for Scenario Set $S3$

Freq	Doppler Spread	RMS Doppler Bandwidth
400MHz	1.977Hz	1.4476 Hz
2.25GHz	2.929Hz	1.8789 Hz
4.5GHz	3.029Hz	1.9861 Hz

Table II lists the Doppler spread based on a scenario set $S3 = \{Freq3, Motion3, TX3, RX3\}$, where $Motion3 = \{Walk\}$, $Freq3 = \{400MHz, 2.25GHz, 4.5GHz\}$, $TX3 = \{LeftAnkle\}$ and $RX3 = \{RightHip\}$. From table II, it comes to the conclusion that the Doppler spread increases with respect to the center frequency of transmission waveform with the same antenna positions and the same type of motion, but not proportionally.

IV. RMS Doppler Bandwidth

A more specific estimation of the Doppler spread is the RMS Doppler bandwidth[3], defined as

$$f_N = \sqrt{\frac{\int \lambda^2 V(\lambda) d\lambda}{\int V(\lambda) d\lambda}}, \tag{2}$$

where $V(\lambda)$ is the Fourier transform of the complex autocorrelation function of $H(f_c;t)$. RMS Doppler bandwidth is proposed to describe the Doppler shift by calculating the

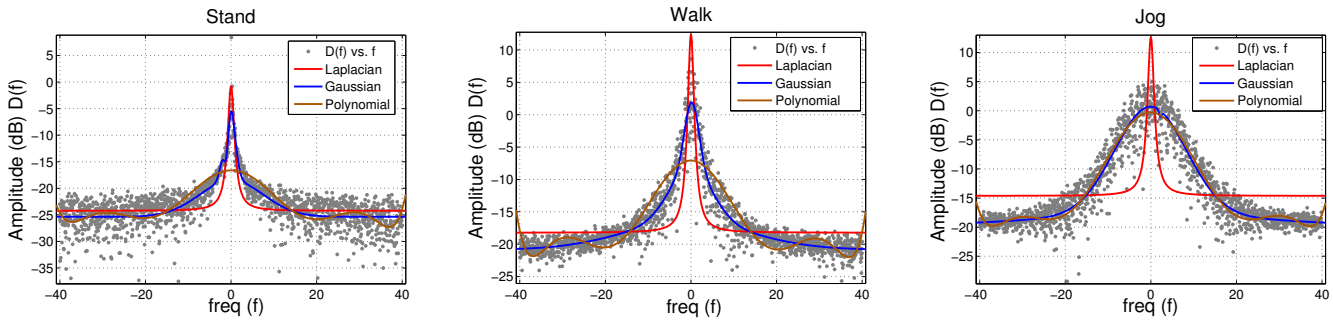

Fig. 3: Shape of Doppler Spread Spectrum for Different Human Body Motions

weighted signal power rather than a simply overall width of the spectrum in a more scientific method.

For the scenario set S, the RMS Doppler Bandwidth ranges from $0.6Hz$ to $4Hz$. The reason for such difference comes from body postures, center waveform frequencies, and antenna positions on the test subject. In table I, for the standing still motion, RMS Doppler bandwidth is always below one, which shows a concentrated distribution of the received signal strength. While for walking and jogging motions, RMS Doppler bandwidth is much larger than that of standing still, and received signal strength is dispersedly distributed in the frequency domain. The Doppler spread in frequency domain in Fig.2 shows the power distribution for scenario $S1$, where the width in frequency and the averaged power distribution keep increasing from (b) to (d). For a specific scenario $S2$ mentioned in section III, table II illustrated that the RMS Doppler spread bandwidth also increases with respect to the center frequency of transmission signal.

V. Shape of Doppler Spread Spectrum

In the on-body to on-body channel, the transmitter and receiver could be either stationary or mobile. The relative mobility will lead to different Doppler spread shapes in frequency domain, where the "Bell-Shaped" Doppler spectrum depends on center frequencies and human body motions. In this study, we obtained maximum likelihood estimates of measured received signal strength (dB) with respect to the frequency in three estimators, which is commonly used to characterize and model fading channels in past researches.

- Laplacian

$$D(f) = \frac{a_1}{a_2 + a_3 f^2} + a_4, \tag{3}$$

  where a_i is the coefficient in the model.

- Gaussian

$$D(f) = \sum_{i=0}^{i=n-1} a_i \exp(-(f - b_i)^2 / c_i^2), \tag{4}$$

  This is an nth order Gaussian model and a_i, b_i and c_i is the coefficients in the model.

- Polynomial

$$D(f) = \sum_{i=0}^{i=n-1} a_i f^i, \tag{5}$$

  This is an nth order Polynomial model and a_i is the coefficient in the model.

In order to compare goodness of these three shape fittings, we consider the Root Mean Square Error (RMSE) between these three functions and the actual measured data as the criteris. Given the measured results and fitting functions, we compare the standard deviation of estimated and measured component by

$$RMSE = \sqrt{MSE(\hat{\theta})} = \sqrt{E((\hat{\theta} - \theta)^2)}, \tag{6}$$

where $\hat{\theta}$ is an optimal estimator of measured results θ giving the least RMSE value. Comparing the RMSE for the Laplacian, Gaussian and Polynomial estimators, we could conclude that a 4-th order Gaussian function is usually a better fitting of median values for a general scenario. Considering scenario set S, the 4-th order Gaussian estimator performs much better than Polynomial and Laplacian estimators for the jogging posture. But it does not always perform better than the other two estimators for the standing and walking postures. There are only 5 out of 45 cases where the Laplacian estimator outperforms the 4-th order Gaussian estimator for the scenario set S. And Laplacian function is usually a poor fitting of the power magnitude for jogging posture. Fig.3 shows a sample of shape fittings for scenario $S1$, where the Gaussian estimator shows a better performance than the Laplacian and Polynomial estimators.

VI. Coherence Time Analysis

Coherence time is the description of time dispersive nature of the fading channel in time domain, equivalent to the Doppler spread in frequency domain. It is the time duration over which the channel could be considered as invariance, and the two signals have a strong power correlation at this time interval. In a baseband transmission, a signal distortion will occur when the bandwidth of the signal is greater than the inverse of coherence time. Coherence time T_m and Doppler spread f_m are inversely proportional to each other, shown in the equation below.

$$f_m = \frac{k}{T_m}, \tag{7}$$

where k is a varying value for different scenarios depending on the correlation value. Channel coherence time is typically

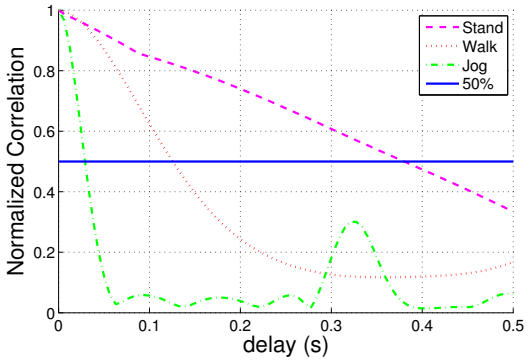

Fig. 4: Coherence Time Analysis for Different Human Body Motions

defined as the time duration over which normalized autocorrelation coefficients of time domain data is above 0.5, defined by

$$\rho(m) = \frac{\sum_{n=1}^{N-|m|} \{x(n+m) - m_x\}\{x^*(n) - m_x^*\}}{|r(n+m)| \times |r(n)|}, \qquad (8)$$

where m_x is the mean value with $m_x = \frac{1}{N}\sum_{n=1}^{N} x(i)$, and $|r(n)| = \sqrt{\frac{1}{N}\sum_{n=1}^{N}[x(n) - m_x]^2}$. The normalized autocorrelation function for scenario $S2$ is shown in figured above. The coherence time for standing, walking and jogging is $T_c = 380.8ms, 125.1ms, 27.07ms$ respectively, which means that a maximum symbol transmission rate of $\frac{1}{T_c} = 2.62Hz, 7.99Hz, 39.94Hz$ individually is required to avoid distortion from the frequency dispersion in digital communication system. Fig.4 shows that the channel of the standing posture has a more stable channel which holds a longer duration and suffers from less temporal variations. On the other hand, the channel of the jogging posture suffers from a deeper fading with a shorter stable duration and a fast changing characteristic feature .

VII. Conclusion

This paper presents the characterization of the on-body time-variant channels based on an extensive measurement champaign at MICS band, ISM band and low UWB. Using a Vector Network Analyzer, the narrowband measurement is performed with the analysis from the Doppler spread aspect. In order to help to design medical sensors which are used to detect body postures in Body Area Network, the Doppler spread, RMS Doppler Bandwidth and coherence time are analyzed thoroughly for different scenarios by considering the center frequencies, antenna positions and body postures. Furthermore, the "bell-shaped" Doppler spread spectrum is fitted into Gaussian function based on the comparison of the Root Mean Squared Error.

References

[1] S.J. Howard, K. Pahlavan, "Fading Results From Narrowband Measurements of the Indoor Radio Channel," in *Personal, Indoor and Mobile Radio Communications*, pp. 92, Sept. 1991.

[2] S.L. Cotton, W.G. Scanlon, "Characterization and modeling of on-body spatial diversity within indoor environments at 868 MHz," in *IEEE Transactions on Wireless Communications*, vol.8, no.1, pp. 14-18, Feb. 2009.

[3] S.L. Cotton, G.A. Conway, W.G. Scanlon, "A Time-Domain Approach to the Analysis and Modeling of On-Body Propagation Characteristics Using Synchronized Measurements at 2.45 GHz," in *IEEE Transactions on Antennas and Propagation*, vol.57, no.4, pp.943, Apr. 2009.

[4] A. Fort, C. Desset,P. De Doncker, P. Wambacq, L. Van Biesen, "An ultra-wideband body area propagation channel Model-from statistics to implementation," in *IEEE Transactions on Antennas and Propagation*, vol.54, no.4, pp. 1820, Jun. 2006 .

[5] D. Smith, L. Hanlen, D. Miniutti, J. Zhang, D. Rodda, B. Gilbert, "Statistical Characterization of the Dynamic Narrowband Body Area Channel," in *Applied Sciences on Biomedical and Communication Technologies*, pp. 1-5, Oct. 2008.

[6] D. Smith, L. Hanlen, J. Zhang, D. Miniutti, D. Rodda, B. Gilbert, "Characterization of the Dynamic Narrowband On-Body to Off-Body Area Channel," in *ICC '09*, pp. 14-18, Jun. 2009.

[7] D. Smith, D. Miniutti, L. Hanlen, D. Rodda and B. Gilbert, "Dynamic Narrowband Body Area Communications: Link-Margin Based Performance Analysis and Second-Order Temporal Statistics," in *IEEE WCNC 2010*, pp. 14-18, Sydney, April 2010.

[8] Bin Zhen, Minseok Kim, Jun-ichi Takada, Ryuji Kohno, "Characterization and modeling of dynamic on-body propagation," in *Pervasive Computing Technologies for Healthcare*, pp.1, UK, Apr. 2009.

[9] Bin Zhen, Minseok Kim, Jun-ichi Takada, Ryuji Kohno , "Finite-State Markov Model for On-Body Channels with Human Movements," in *ICC 2010*, pp.1, May 2010.

[10] A. G. Dimakis, V. Prabhakaran, and K. Ramchandran, "Fading Results From Narrowband Measurements of the Indoor Radio Channel," in *IPSN*, April 2005, pp. 111–117.

[11] A. Fort, C. Desset, P. Wambacq, L.V. Biesen, "Indoor body-area channel model for narrowband communications," in *IET Microwaves, Antennas and Propagation*, vol.1, pp.1197, Dec. 2007.

[12] S. Stein, "Fading Channel Issues in System Engineering," in *Selected Areas in Communications, IEEE Journal on Communications*, vol.5, Issue.2, pp.68, Jan. 2003.

[13] Liu Lingfeng, P. De Doncker, C. Oestges, "Fading Correlation Measurement and Modeling on the Front Side of a Human Body," in *Antennas and Propagation, EuCAP*, pp.969, Mar. 2009.

[14] D.B. Smith, J. Zhang, L.W. Hanlen, D. Miniutti, D. Rodda, B. Gilbert, "Temporal Correlation of the Dynamic On-Body Area Radio Channel," in *Electronics Letters*, vol.45, pp.1212, Sept. 2009.

[15] Zhang Jian, D.B. Smith, L.W. Hanlen, D. Miniutti, D. Rodda, B. Gilbert, "Stability of Narrowband Dynamic Body Area Channel," in *IET Microwaves, Antennas and Propagation*, vol.8, pp.53 - 56, Nov. 2009.

[16] K. Sayrafian-Pour, Wen-Bin Yang, J. Hagedorn, J. Terrill, K.Y. Yazdandoost, "A Statistical Path Loss Model for Medical Implant Communication Channels," in *Personal, Indoor and Mobile Radio Communications* , pp.2995 - 2999, Sept. 2009.

[17] R. Ganesh, K. Pahlavan, "Statistical Modelling and Computer Simulation of Indoor Radio Channel," in *Communications, Speech and Vision, IEEE Proceedings Communications*, vol.138, Issue 3, pp.153, Aug. 2002.

[18] Hao Yang, A. Alomainy, Zhao Yan, C.G. Parini, Y. Nechayev, P. Hall, C.C. Constantinou, "Statistical and Deterministic Modelling of Radio Propagation Channels in WBAN at 2.45GHz," in *Antennas and Propagation Society International Symposium*, pp.2169, Jul. 2006.

[19] Raffaele DErrico, Laurent Ouvry, "A Statistical Model for On-Body Dynamic Channels," in *International Journal of Wireless Information Networks*, vol.17, pp.92-104, Jan. 2010.

[20] K. Y. Yazdandoost and K. Sayrafian-Pour, Channel Model for Body Area Network (BAN). IEEE P802.15-08-0780-09-0006, April, 2009

[21] R. Cutler, L.S. Davis, "Robust real-time periodic motion detection, analysis, and applications", in *IEEE Transactions on Pattern Analysis and Machine Intelligence*, vol. 22, pp. 781-796, Aug. 2000.

[22] M. Quwaider, S. Biswas, "Body Posture Identification using Hidden Markov Model with a Wearable Sensor Network", in *BODYNETS 2008*, March 2008.